Supplementary Material

The property–efficiency relationship over Rh/Ga_xNb_y catalysts in photothermal dry reforming of CH_4

Yuqiao Li[a+], Shaoyuan Sun[a+], Dezheng Li[a*], Huimin Liu[a*], Yiming Lei[a,b*]

[a], School of Chemical and Environmental Engineering, Liaoning University of Technology, 121001 Jinzhou, P. R. China

[b], Departament de Química (Unitat de Química Inorgànica), Facultat de Ciències, Universitat Autònoma de Barcelona (UAB), Cerdanyola del Valles, 08193 Barcelona, Spain

+, these authors contributed equally to the manuscript.

Corresponding authors

Dezheng Li, email: ldz221882002@163.com

Huimin Liu, email: liuhuimin08@tsinghua.org.cn

Yiming Lei, email: 1689472@uab.cat

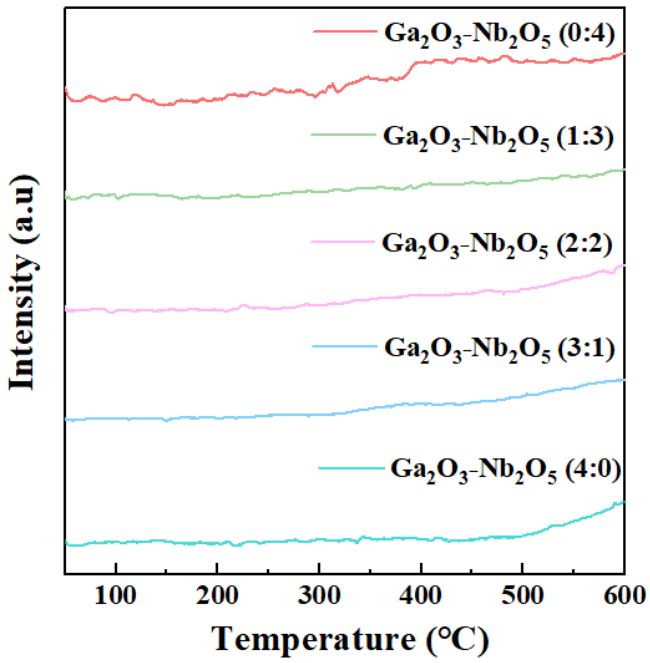

Figure S1. H_2-TPR results of Ga_2O_3-Nb_2O_5 precursors.

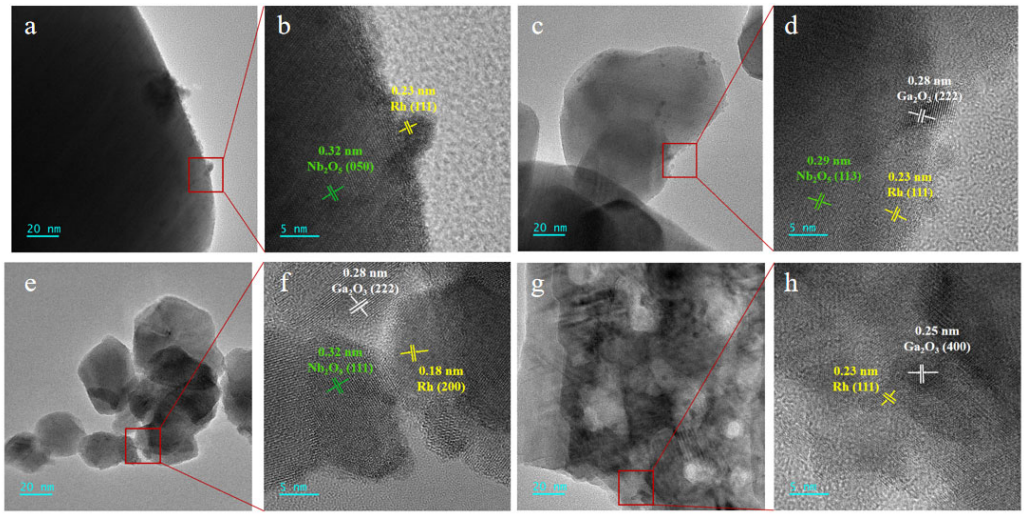

Figure S2. TEM and HR-TEM images of (a and b) Rh/Ga_1Nb_3, (c and d) Rh/ Ga_2Nb_2, (e and f) Rh/ Ga_3Nb_1, and (g and h) Rh/ Ga_4Nb_0.

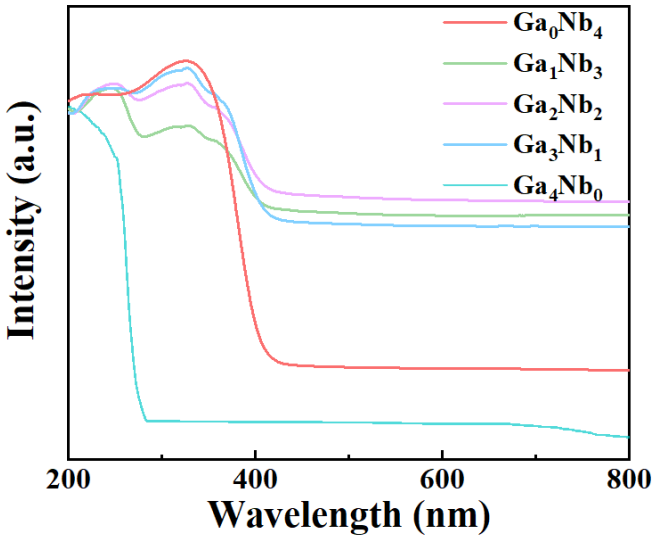

Figure S3. UV-vis spectra of Ga_xNb_y catalysts.

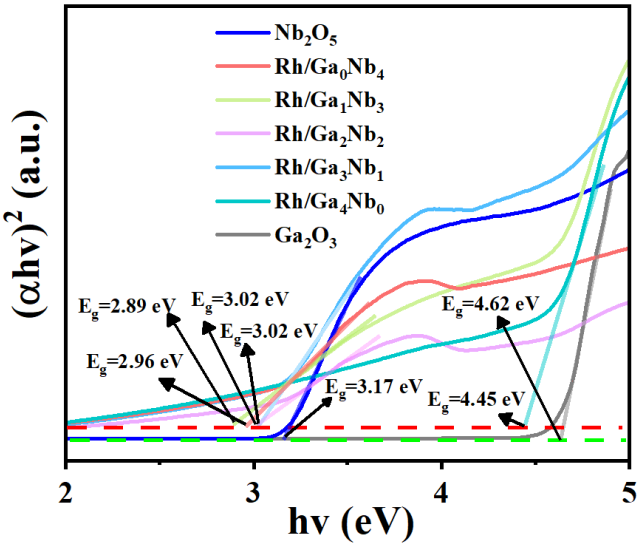

Figure S4. Tauc plots and bandgap of Rh/Ga_xNb_y catalysts.

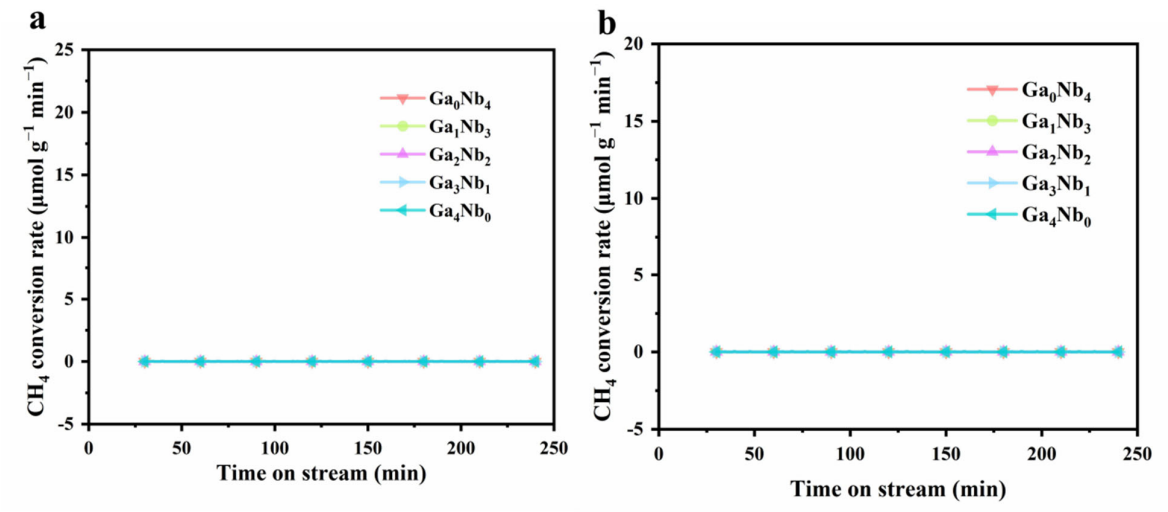

Figure S5. Photothermal catalytic efficiency of Ga_xNb_y in photothermal DRM reaction system. (a) CO_2 conversion and (b) CH_4 conversion. Reaction conditions: 500 ℃, CH_4 : CO_2 = 1 : 1, total flow rate: 10 mL·min^{-1}, 0.10 g of Ga_xNb_y catalyst, with visible light irradiation (300 W Xe lamp, $\lambda > 420$ nm).

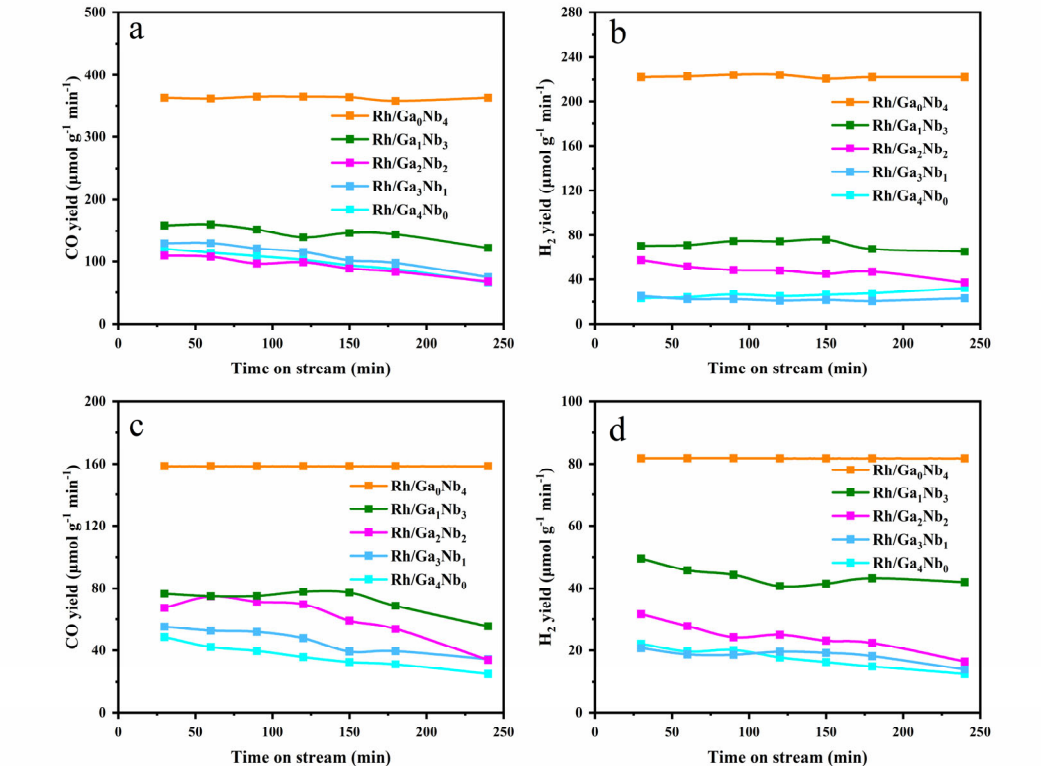

Figure S6. Photothermal catalytic efficiency of Rh/Ga_xNb_y in photothermal DRM reaction system. (a) CO yield and (b) H_2 yield. Reaction conditions: 500 °C, CH_4 : CO_2 = 1 : 1, total flow rate: 10 mL·min^{-1}, 0.10 g of Rh_2O_3/Ga_xNb_y catalyst, with visible light irradiation (300 W Xe lamp, $\lambda > 420$ nm). Thermal catalytic efficiency of Rh/Ga_xNb_y in thermal-driven DRM reaction. (c) CO yield and (d) H_2 yield. Reaction conditions: 500 °C, CH_4 : CO_2 = 1 : 1, total flow rate: 10 mL·min^{-1}, 0.10 g of Rh_2O_3/Ga_xNb_y catalyst, without visible light irradiation.

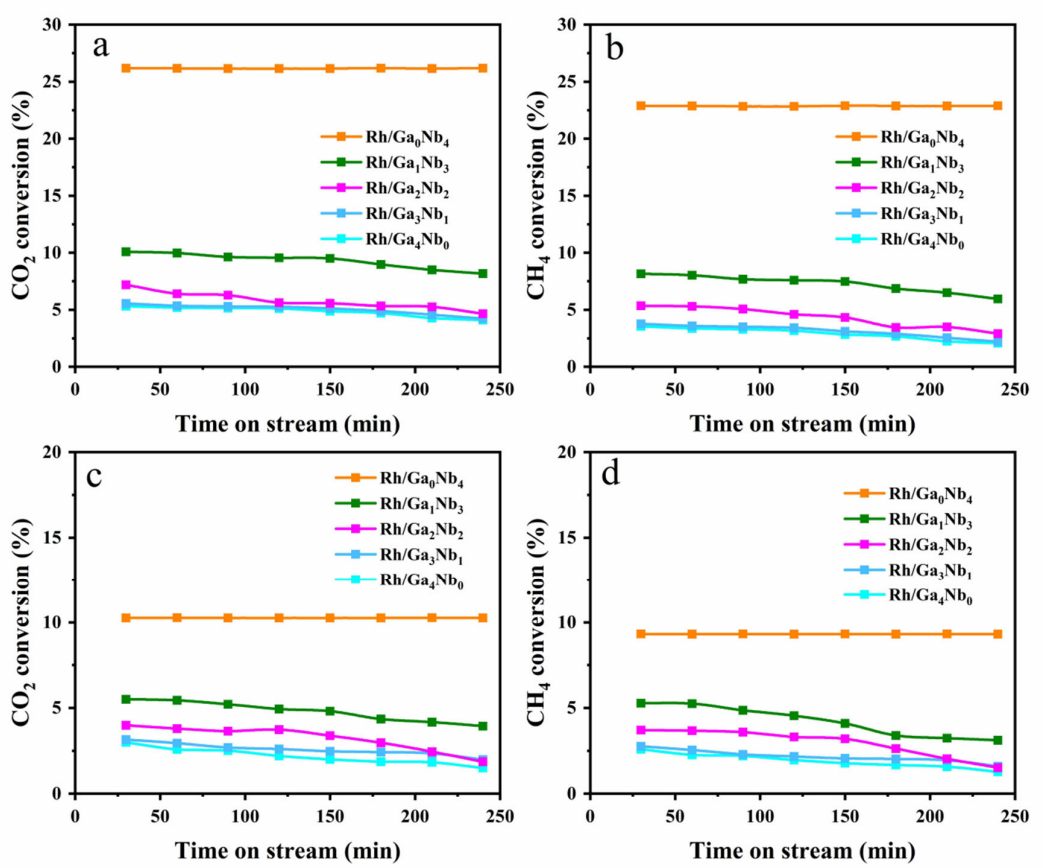

Figure S7. Photothermal catalytic efficiency of Rh/Ga_xNb_y in photothermal DRM reaction system. (a) CO_2 conversion and (b) CH_4 conversion. Reaction conditions: 500 ℃, CH_4 : CO_2 = 1 : 1, total flow rate: 10 $mL \cdot min^{-1}$, 0.10 g of Rh_2O_3/Ga_xNb_y catalyst, with visible light irradiation (300 W Xe lamp, $\lambda > 420$ nm). Thermal catalytic efficiency of Rh/Ga_xNb_y in thermal-driven DRM reaction. (c) CO_2 conversion and (d) CH_4 conversion. Reaction conditions: 500 ℃, CH_4 : CO_2 = 1 : 1, total flow rate: 10 $mL \cdot min^{-1}$, 0.10 g of Rh_2O_3/Ga_xNb_y catalyst, without visible light irradiation.

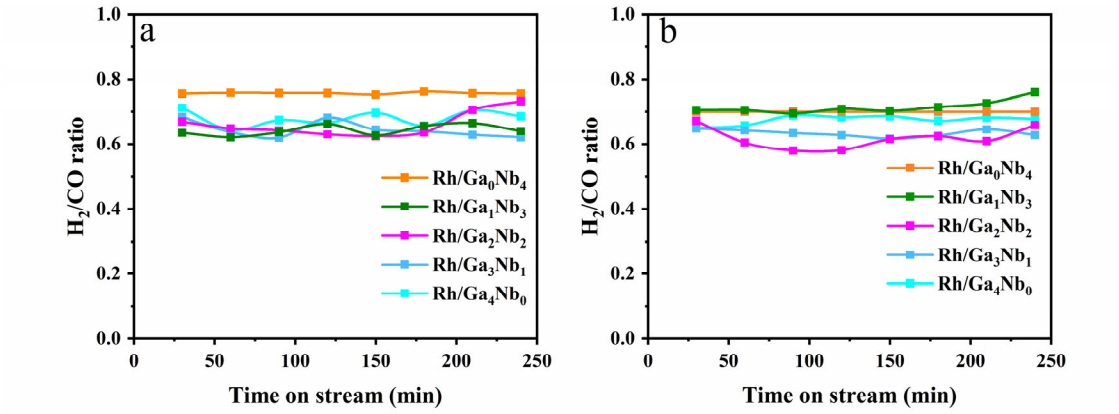

Figure S8. H_2/CO ratio over all catalysts. (a) photothermal, (b) thermal catalysis. Reaction conditions: CH_4/CO_2 = 1: 1, total flow rate: 10 mL· min^{-1}, 0.10 g of catalyst, with visible light irradiation (300 W Xe lamp, λ > 420 nm).

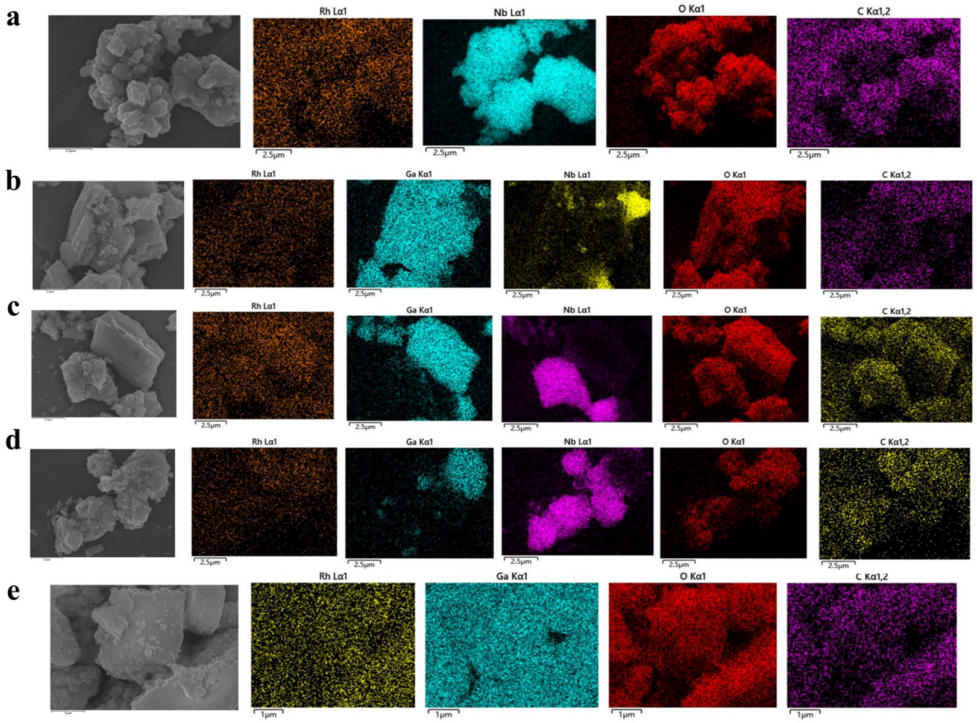

Figure S9. SEM image and EDX mapping of the catalyst after 4 h of photothermal DRM reaction. (a) Rh/Ga_0Nb_4, (b) Rh/Ga_1Nb_3, (c) Rh/Ga_2Nb_2, (d) Rh/Ga_3Nb_1, and (e) Rh/Ga_4Nb_0.

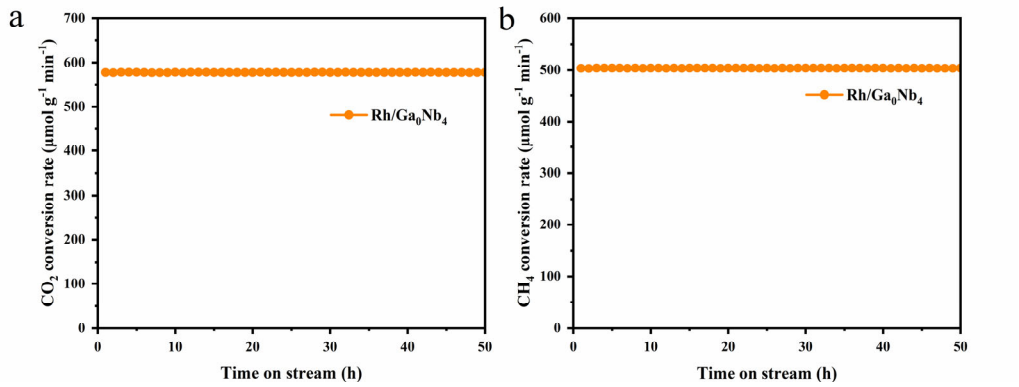

Figure S10. Photothermal catalytic efficiency of Rh/Ga_xNb_y in photothermal DRM reaction system. (a) CO_2 conversion and (b) CH_4 conversion. Reaction conditions: 500 ℃, CH_4 : CO_2 = 1 : 1, total flow rate: 10 mL·min^{-1}, 0.10 g of Rh_2O_3/Ga_xNb_y catalyst, with visible light irradiation (300 W Xe lamp, $\lambda > 420$ nm).

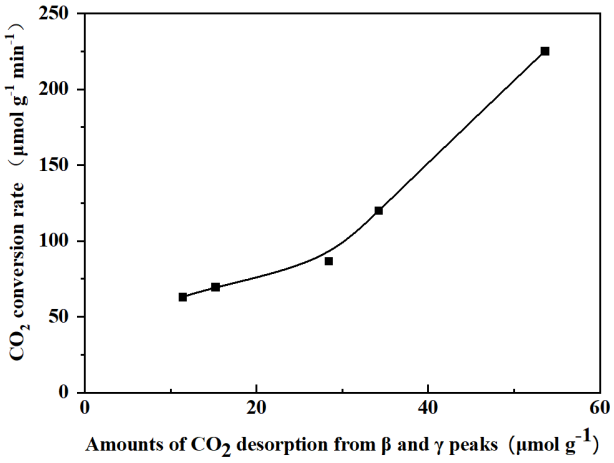

Figure S11. The catalytic efficiency of Rh/Ga_xNb_y in thermally driven DRM is related to the CO_2 desorption capacity of the β and γ peaks.



Figure S12. Photoelectrochemical efficiency evaluation system.

Table S1. Comparison table of thermal and photothermal catalysts for DRM reactions.

Catalysts	**Reaction conditions**	**T(°C)**	**Catalytic performance (μmol·g^{-1}·min^{-1})**		**Ref.**
			CO_2	**CH_4**	
Rh/Ga_0Nb_4	Photothermal	500	578.0	504.0	This work
Rh-Au/SBA-15	Photothermal	500	60.0	53.3	[1]
Pt-Au/SiO_2	Photothermal	400	68.6	54.5	[2]
Pt/Ta_2O_5	Photothermal	600	310.0	280.0	[3]
Ni@SiO_2-yolk	Photothermal	400	510	480	[2]
$Pd_{90}Au_{10}/Al_2O_3$	Photothermal	500	1210.6	930.3	[4]
10Ni/CaAlO	Thermal	600	91.1	93.8	[5]

$NiFe/Al_2O_3$	Thermal	450	125.0	98.2	[6]
2Ni–R	Thermal	500	178.0	52.5	[7]
HT5	Thermal	600	575.0	361.6	[8]
Pd/Nb_2	Thermal	750	1984.1	1500.0	[9]

References

1. Liu, H.; Meng, X.; Dao, T. D.; Zhang, H.; Li, P.; Chang, K.; Wang, T.; Li, M.; Nagao, T.; Ye, J., Conversion of carbon dioxide by methane reforming under Visible-Light irradiation: Surface-Plasmon-Mediated nonpolar molecule activation. *Angew Chem Int Edit.* **2015**, *54*, 11545-11549.

2. Song, H.; Meng, X.; Dao, T. D.; Zhou, W.; Liu, H.; Shi, L.; Zhang, H.; Nagao, T.; Kako, T.; Ye, J., Light-Enhanced carbon dioxide activation and conversion by effective plasmonic coupling effect of Pt and Au nanoparticles. *ACS Appl Mater Inter* **2018**, *10*, 408-416.

3. Ji, G.; Wu, S.; Song, X.; Meng, L.; Jia, Y.; Tian, J., Recent progress in Photo-Thermal synergistic catalysis for methane dry reforming. *Int J Hydrogen Energy* **2024**, *57*, 696-708.

4. Liu, H.; Li, M.; Dao, T. D.; Liu, Y.; Zhou, W.; Liu, L.; Meng, X.; Nagao, T.; Ye, J., Design of PdAu alloy plasmonic nanoparticles for improved catalytic performance in CO_2 reduction with visible light irradiation. *Nano Energy.* **2016**, *26*, 398-404.

5. Yabe, T.; Yamada, K.; Murakami, K.; Toko, K.; Ito, K.; Higo, T.; Ogo, S.; Sekine, Y., Role of electric field and surface protonics on Low-Temperature catalytic dry

reforming of methane. *ACS Sustain Chem Eng.* **2019**, *7*, 5690-5697.

6. Song, Z.; Wang, Q.; Guo, C.; Li, S.; Yan, W.; Jiao, W.; Qiu, L.; Yan, X.; Li, R., Improved effect of Fe on the stable NiFe/Al_2O_3 catalyst in Low-Temperature dry reforming of methane. *Ind Eng Chem Res.* **2020**, *59*, 17250-17258.

7. Lorber, K.; Zavašnik, J.; Arčon, I.; Huš, M.; Teržan, J.; Likozar, B.; Djinović, P., CO_2 activation over nanoshaped CeO_2 decorated with nickel for Low-Temperature methane dry reforming. *ACS Appl Mater Inter* **2022**, *14*, 31862-31878.

8. Ramon, A. P.; Li, X.; Clark, A. H.; Safonova, O. V.; Marcos, F. C.; Assaf, E. M.; Bokhoven, J. A. v.; Artiglia, L.; Assaf, J. M., *In Situ* study of Low-Temperature dry reforming of methane over $La_2Ce_2O_7$ and $LaNiO_3$ mixed oxides. *Appl Catal B-Environ* **2022**, *315*, 121528.

9. Ballesteros-Plata, D.; Infantes-Molina, A.; Rodríguez-Castellón, E.; Cauqui, M. A.; Yeste, M. P., Improving noble metal catalytic activity in the dry reforming of methane by adding niobium. *Fuel* **2022**, *308*, 121996.